2009 IEEE 11th International Conference on Rehabilitation Robotics
Kyoto International Conference Center, Japan, June 23-26, 2009

Design of a Reconfigurable Ankle Rehabilitation Robot and Its Use for the Estimation of the Ankle Impedance

Aykut Cihan Satici Ahmetcan Erdogan Volkan Patoglu

Abstract— **This paper presents the design, analysis, and a clinical application of a reconfigurable, parallel mechanism based, force feedback exoskeleton for the human ankle. The device can either be employed as a balance/proprioception trainer or configured to accommodate range of motion (RoM)/strengthening exercises. The exoskeleton can be utilized as a clinical measurement tool to estimate dynamic parameters of the ankle and to assess ankle joint properties in physiological and pathological conditions. Kinematic analysis and control of the device are detailed and a protocol for utilization of the exoskeleton to determine ankle impedance is discussed. The prototype of the device is also presented.**

I. INTRODUCTION

Assistance of repetitive and physically involved rehabilitation exercises using robotic devices not only helps eliminate the physical burden of movement therapy for the therapists, but also decreases application related costs. Moreover, robot-mediated rehabilitation therapy allows quantitative measurements of patient progress and can be used to realize customized, interactive treatment protocols. This paper presents a novel rehabilitation exoskeleton for patients who have suffered injuries that affect the function of their lower extremities, specifically their ankle movements.

The aim of rehabilitation is to recover physical, sensory and neural capabilities of the patients that were impaired due to an illness or injury. Ankle rehabilitation is commonly necessitated after sprained ankles, one of the most common injuries in sports and daily life [1]. Loss of functional ability, inability to bear weight, and joint instability at the ankle are also experienced after neurological injuries secondary to stroke and contracture deformity secondary to cerebrovascular disease. Physiotherapy exercises are indispensable to regain range of motion (RoM) of the joint, to help restrengthen muscles to bear weight, to promote better awareness of joint position (proprioception), to ensure neural integrity, and to recover dynamic balance.

Recognizing the need for robot assisted rehabilitation devices for ankle physiotherapy, several designs have been proposed to date. Girone *et al.* proposed a force feedback interface, named Rutgers Ankle, based on a Stewart platform [2]. In [3], a virtual reality based interactive training protocol was implemented using the Rutgers Ankle for orthopedic rehabilitation. Home-based remote ankle rehabilitation was addressed in [4], while in [5] the system was extended to a dual Stewart platform configuration to be used for gait simulation and rehabilitation.

In [6], Dai *et al.* proposed another robotic device to treat sprained ankle injuries. Unlike the Stewart platform based design, this device possesses just enough degrees of freedom (DoF) to cover the orientation workspace of the human ankle. The kinetostatic analysis presented in this reference emphasized the importance of employing a center strut to achieve higher stiffness from the device. In [7], Agrawal *et al.* proposed an ankle-foot orthosis for robot assisted rehabilitation and presented the kinematic analysis and the control of the proposed mechanism. Syrseloudis and Emiris studied the translational and rotational RoM of human ankle and foot through human subject experiments, and concluded that a parallel tripod mechanism with an additional rotational axis in series is the most relevant kinematic design to comply with human ankle related foot kinematics [8]. In [9] Yoon and Ryu proposed a hybrid four DoF parallel mechanism based footpad device and presented the kinematic analysis of the novel device. In [10], this work was extended to allow for reconfiguration of the device to support several distinct exercise modes. Moreover, in [11] Anklebot was proposed by Roy *et al.* to aid recovery of the ankle function. A mechanism similar to Anklebot, but with spring over muscle actuators, has also been implemented [12]. Anklebot can be used to measure the ankle stiffness, which is a strong biomechanical factor for locomotion.

There exists a vast amount of literature on the importance of the ankle parameters during locomotion [13], [14]. Many diagnostics studies distinguish among passive, intrinsic, and active impedance of the ankle. In particular, ankle dynamic impedance is decomposed into reflex and non-reflex components, while the non-reflex impedance itself has two components: passive, which corresponds to inertial and the visco-elastic properties of the joint, and intrinsic, which is related to the mechanical properties of active muscle [15]. In [16], the dynamic ankle stiffness is evaluated for patients with spinal cord injury and it has been concluded that these patients possess a higher reflex stiffness. Similarly, in [17] spasticity is shown to result in a major alteration of normal muscle-joint anatomical relationship. In particular, ankle extensors, in patients with spastic hemiparesis, are shown to have a much higher intrinsic stiffness even though they may have a normal reflex stiffness. In [18], spastic and contralateral legs of spastic hemiparesis patients are examined and the stiffness of spastic leg is shown to be significantly larger than the stiffness of the contralateral leg, mainly due to the higher passive stiffness of the spastic leg.

A. Erdogan, A. C. Satici, and V. Patoglu are with the Faculty of Engineering and Natural Sciences, Sabancı University, 34956 Istanbul, Turkey. {acsatici,ahmetcan}@su.sabanciuniv.edu, vpatoglu@sabanciuniv.edu

Parallel to these results, in [19], passive, intrinsic, and reflex-mediated mechanical stretch response of the ankle extensors and flexors are evaluated for spastic multiple sclerosis patients. For ankle flexors, passive and intrinsic stiffness values increased with zero reflex-mediated stiffness. On the other hand, for ankle extensions reflex and intrinsic stiffness stay relatively unchanged with a higher passive stiffness.

Ankle stiffness measurements are also used to diagnose aging disorders. In [20], effects of aging on ankle stiffness is pointed out and stepping down movement is analyzed with respect to ankle stiffness. The study concluded that different torque patterns and lower dynamic ankle stiffness are observed in elderly people while stepping down and that an altered control method is used by such subjects while stepping down.

The cited studies emphasize the importance of robust and repeatable measures of ankle properties for diagnosing pathological conditions and for better understanding of health disorders. Unfortunately, currently, most clinical measures of intrinsic joint properties depend on subjective assessment by clinicians and lack quantitative basis and repeatability. Moreover, most of the existing measurement devices cannot account for the complex kinematics of the ankle and can only provide aggregate measurements around a single axis of foot rotation [21], [22], [23]. However, Hertel *et al.* [24] pointed out that, the complex mechanics of the ankle joint is strongly related to acute and chronic ankle instability and the kinematics of the ankle must be considered for evaluating and treating ankle injuries effectively. The ankle rehabilitation robots developed in [4] and [10] have higher DoF and are proposed for administering physical therapy exercises as well as evaluating ankle properties. However, no formal protocols for estimation of ankle stiffness have been covered in these studies. Finally, [11] presents a device used for ankle impedance estimation and has three (two active and one passive) DoF. However, within the natural RoM of the ankle, the kinematics of this device conflicts with the kinematics of the human ankle; hence, the device can only provide aggregate measurements of impedance along its own joint axes.

In this paper, the design, analysis, and application potential of a reconfigurable, parallel mechanism based ankle exoskeleton are presented. Similar to the references [10] and [25], reconfigurability is built into the design such that the device can be arranged to administer ROM/strengthening exercises while sitting and to support balance/proprioception exercises while standing. The reconfigurable kinematics of the design not only supports different types of exercises but also allows the exoskeleton to be employed as a clinical measurement tool that can precisely monitor joint movements and torques at the human ankle. In particular, the exoskeleton can be exploited to estimate intrinsic kinematical and mechanical properties of the human ankle about its rotation axes, allowing assessment of ankle joints in physiological and pathological conditions.

II. DESIGN OF THE ANKLE EXOSKELETON

A. Determination of the Kinematic Structure(s)

Kinematics of the human ankle, which allows plantarflexion/dorsiflexion, abduction/adduction, and inversion/eversion is quite complex. Many studies make use of a simplified three DoF spherical joint model for the ankle joint, in which the axes of rotation for these three motions are assumed to coincide at a single point on the ankle [6], [26]. In this paper, a model that is verified by and commonly utilized in the biomechanics literature is adapted to study the kinematics of the human ankle [8]. This model recognizes the coupled motion of the foot and hypothesizes that the ankle joint can be modeled as a spatial serial kinematic chain with two revolute joints (RR): an upper ankle joint that supports the rotational dorsiflexion/plantarflexion motion and a subtalar joint that supports the rotational supination/pronation motion. Supination/pronation rotation is a complex motion that has both inversion/eversion and abduction/adduction components. The exact motion of the ankle shows wide variation among humans, as this motion depends on size and orientation of foot bones, shape of articulated surfaces and constraints imposed by ligaments, capsules, and tendons. Workspace and torque limits of human ankle are given in Table I based on [10]. Statistical data on human foot and ankle sizes can be found in [27].

TABLE I
WORKSPACE AND TORQUE LIMITS OF HUMAN ANKLE

Joint	Joint Torque Limits	Designed Torque Limits	Joint RoM	Designed RoM
Dorsiflexion\	40.7–97.6 Nm	100 Nm	20°	40°
Plantarflexion	20.3–36.6 Nm	50 Nm	40°	40°
Inversion\	max 48 Nm	50 Nm	35°	35°
Eversion	max 34 Nm	50 Nm	25°	35°

A kinematic chain that is suitable to serve as an exoskeleton should allow for and support natural movements of the human joints when the device is worn by an operator. To ensure safety, to allow for small joint misalignments and modeling imperfections, couplings between the exoskeleton and the operator are designed to be elastic. Elasticity allows for the relative motion of the human limb with respect to the device when the kinematics of the device is in conflict with the natural motion of the ankle. However, it is still desirable to have the exoskeleton to possess kinematics that is compatible with the human ankle motions so that the motion of the ankle can be closely controlled during the therapy. Hence, kinematic structures that closely meet the ergonomy requirement are preferred.

Once the ergonomy requirement is met, the choice of closed kinematic chains (parallel mechanisms) is preferable over the choice of serial mechanisms in satisfying requirements of force feedback applications. Specifically, parallel mechanisms offer compact designs with high stiffness and have low effective inertia since their actuators can be grounded or placed on parts of the mechanism that experience low accelerations. In terms of dynamic performance, high position and force bandwidths are achievable with parallel mechanisms thanks to their light but stiff structure.

In order to span the whole natural range of motion of the human ankle and to do so robustly for various operators of different ankle and foot dimensions (kinematics), an underactuated 3UPS[1] parallel mechanism is proposed as the kinematic structure of the exoskeleton. A 3UPS mechanism has six DoF that can be designed to cover the whole RoM of the human ankle and foot. Even though the human ankle can be modeled with two revolute joints, the exoskeleton design requires more than two DoF to cover the whole RoM of the ankle, since, in general, it is not possible to perfectly align the joint axes of the ankle with the joint axes of the device. Having only three actuators, the 3UPS mechanism is underactuated; however, when worn by a human operator, the kinematics of the human ankle becomes a part of the exoskeleton. Coupled to the human operator, the 3UPS exoskeleton operates as a 3UPS-RR kinematic structure with two independent degrees of freedom, dictated by the kinematics of the human ankle. Hence, not only can the device cover the whole RoM of any operator, but can do so in a completely ergonomic manner. Moreover, even when the operator is completely passive, the two DoF 3UPS-RR device has three actuated joints and is a redundant mechanism. This redundancy can be exploited to avoid singularities of the device.

Employing the human ankle as a part of the kinematic chain, the 3UPS-RR configuration is useful for RoM/strengthening exercises; however, this kinematic structure is not preferable for balance/proprioception exercises, since the forces/torques transferred to the ankle joint cannot be supported. Moreover, an exoskeleton need not cover the whole RoM of the ankle for balancing exercises. To support to the human weight and to adjust the torques transferred to the ankle joints while covering an acceptable portion of the natural human ankle workspace, a 3RPS-R parallel mechanism is proposed as the kinematic structure of the exoskeleton for balancing exercises. The 3RPS-R mechanism is first utilized as a wrist exoskeleton by Gupta *et al.* [28] and adapted as a wrist rehabilitation device in [29]. The optimal design of 3RPS-R mechanism for force feedback applications is addressed in [30] and [31].

The underactuated 3RPS-R mechanism has four DoF and three prismatic actuators. When worn by an operator, the kinematics of the human ankle becomes redundant and the 3RPS mechanism dictates the kinetostatics of the coupled system. Addition of a passive revolute joint (R) to the base platform of the 3RPS allows for the internal/external rotations of the foot, recovering the most of the useful workspace during balancing exercises. The four DoF 3RPS-R can be easily programmed to trace trajectories that comply well with the natural movements of the human ankle. For instance, during walking the human ankle typically undergoes a maximum of 6° of subtalar axis rotation and 17° of ankle axis rotation [32]. During such a motion, typical discrepancy between the human ankle motion and the 3RPS-R motion stays below 5mm, an amount that can be easily tolerated by the elastic couplings used. Hence, utilization of a passive revolute joint at the base platform, customized trajectories of the device, and compliant couplings can ensure ergonomic device movements for balancing exercises.

In this study, a reconfigurable mechanism that can serve both as the 3RPS-R and the 3UPS mechanisms is selected as the kinematic structure of the ankle exoskeleton. Being compact and wearable, and allowing for the movements of the human ankle without collisions with the device, these two parallel mechanisms are suitable to serve as wearable force feedback devices.

B. Dimensioning and Implementation

Imperative design requirements every exoskeleton must satisfy include ensuring safety and complying with the ergonomic needs of the human operator. Safety is assured by the recruitment of back-drivable actuators with force/torque limits implemented in software. In particular, highly back-driveable direct drive linear actuators are utilized in the prototype. The use of series elastic actuators are envisioned for a later prototype, since these actuators can achieve improved force output-weight ratios with sufficiently low output impedances. The ergonomy of the design is considered at the kinematic synthesis level. The 3UPS configuration of the exoskeleton allows for ergonomic motion of human ankle over its whole RoM, since the ankle itself is a part of the kinematic structure. The 3RPS configuration works in a predetermined workspace that covers a large portion of the ankle workspace. The absence or avoidance of singularities within the workspace is another imperative design requirement the mechanisms need to satisfy. The workspace of the 3RPS mechanism is selected to be free of singularities, while the redundant nature of 3UPS-RR kinematic structure is exploited for singularity avoidance.

Since the performance of parallel mechanisms is highly sensitive to their dimensions, optimization studies are absolutely necessary for design of these types of mechanisms [33]. For a rehabilitation device that needs to bear human weight, the utilization from the actuators and the stiffness of the device should be maximized such that for highest torque outputs and rigidity can be achieved from the actuators available. In [34], authors present the optimal dimensional synthesis of the reconfigurable ankle exoskeleton mechanisms with respect to multiple design criteria. In particular, optimal performance of the device is quantified by studying the scaled kinematic Jacobian matrix over the entire workspace. Then, multi-criteria optimization of the 3RPS parallel mechanism is addressed using the framework introduced in [35], [36]. The average value of the kinematic isotropy index is chosen to characterize actuator utilization, while the minimum value of the minimum singular value is kept as high as possible over the workspace. For scaling of the Jacobian matrix, the non-uniform force/torque requirements of the human ankle, given in Table I, are mapped to uniform forces at the joint space, since the actuators are selected to be identical. The readers are referred to [34] for

[1]Parallel mechanisms are commonly denoted by using symbols U, R, S, and P, which stand for universal, revolute, spherical, and prismatic joints. Symbols corresponding to actuated joints are underlined in this notation.

the details of the optimal dimensional synthesis of the ankle exoskeleton.

Reconfigurability is built into the design thanks to extensive similarities between the two parallel mechanisms. The reconfiguration of the parallel manipulator to achieve different kinematic configurations, hence DoF, is achieved using interchangeable passive joint modules, as suggested in [37]. The final design is similar to [25] in that reconfiguration is used to support both RoM/strengthening and balance/proprioception exercises. In our device, the reconfigurability is obtained using the lockable universal joints shown in Figure 1. When the joint is unlocked, series of revolute joints function as a universal joint rotating about the desired axes. When the second joint axis is locked using a bolt, the locked universal joint is constrained to function as a revolute joint, that free to rotate only about the first axis. Hence, the lockable universal joint allows a 3UPS mechanism to be reconfigured into a 3RPS mechanism, and visa versa.

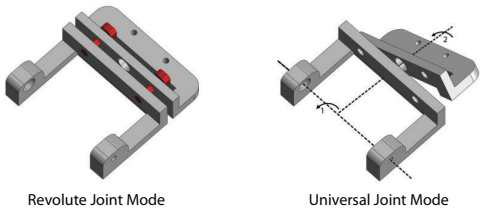

Fig. 1. Reconfigurable universal/revolute joint

In the final design, it is desirable to have a device that is wearable and portable, especially during balance/proprioception exercises. Using the optimal dimensions obtained in [34], choosing 6061 aluminum as the material used for the links, and utilizing commercial direct drive linear motors, the overall device weighs 5.35kg, 3.75kg of which is due to the three linear actuators. The weight of the device is distributed over the upper leg and the upper mid-calf using tight straps around the knee as shown in Figure 2. Weight can further be distributed over the body by suspending the device from the shoulder of the operator, as done in [11].

The final design of the reconfigurable ankle rehabilitation robot, named *SUkorpion AR* after **S**abanci **U**niversity **K**inetostatically **O**ptimized **R**econfigurable **P**arallel **I**nterface **on** **A**nkle **R**ehabilitation, is presented in Figure 2. Finally, in Figure 3 the prototype of the device is presented.

III. Analysis, Control, and Clinical Use of the Ankle Exoskeleton in the 3UPS Mode

A. Estimation of Ankle Parameters

The determination of intrinsic biomechanical parameters of the ankle is a challenge since these parameters show wide variation among humans, as they depend on size and orientation of foot bones, shape of articulated surfaces, and constraints imposed by ligaments, capsules, and tendons. In order to provide a protocol to estimate ankle properties, the kinematics and kinetics of the human ankle, the exoskeleton in the 3UPS mode, and the coupled human-exoskeleton system need to be studied. In this section, first we overview these analyses and present a simulation of the coupled device

Fig. 2. The design of *SUkorpion AR*

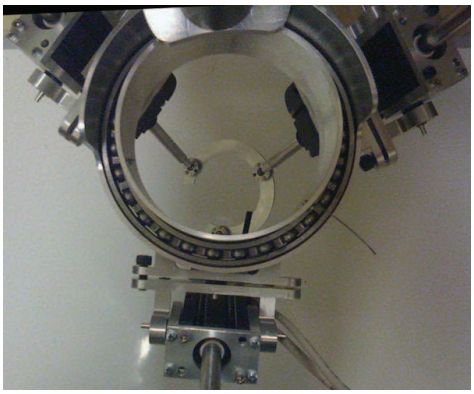

Fig. 3. An early prototype of *SUkorpion AR*

kinematics. These kinematic analyses characterize the mappings among measured quantities and the apparent motion of and forces/torques at *both* the foot and the ankle joint. Next, the controller and the measurement protocol designed to estimate ankle impedance are explained. Estimation of the axes of rotation and the dynamic impedance of the ankle are detailed and simulation results are presented.

B. Kinematics of the Coupled Human-Exoskeleton System

When the patient is attached to the exoskeleton configured in the 3UPS mode, the human ankle becomes a part of the kinematic structure; hence, kinematics of human ankle is required to be considered in the analysis of the coupled human-exoskeleton system. In particular, human ankle imposes independent constraints to the 3UPS mechanism and the coupled system possesses the kinematics of a 3UPS-RR mechanism as depicted in Figure 4. A 3UPS-RR consists of six bodies: a base platform N, three extensible links R, S, T, a center link A, and a moving platform W. The end-effector is worn by the operator; hence, the foot is (almost) rigidly

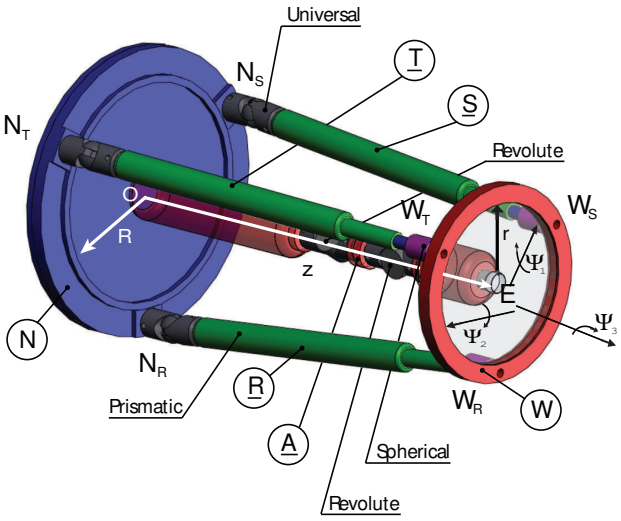

Fig. 4. 3UPS-RR mechanisms in perspective view

attached to the moving platform W. The ankle of the operator is modeled as two revolute joints in series (RR) and the upper mid-calf of the operator is fixed to the base platform N. Extensible links of the exoskeleton are connected to the base platform via universal joints, while the rotating platform is connected to the extensible links by means of spherical joints. In this paper, the analysis is limited to a symmetric 3UPS-RR mechanism where the universal joints and the spherical joints are spaced at 120° along the circumference of the base platform of radius R and the moving platform of radius r, respectively.

The 3UPS-RR mechanism has two DoF corresponding to a coupled motion of the moving platform W with respect to the fixed reference frame N. The lengths of the extensible links are actuated to control these DoF. Even when human operator is completely passive, the two DoF 3UPS-RR structure has three actuated joints; hence, is a redundant mechanism.

Forward and inverse kinematics of the 3UPS-RR mechanism can be addressed by studying the kinematics of the 3UPS mechanism and the spatial serial RR mechanism, separately. Letting x, y, z, ψ_1, ψ_2, and ψ_3 to denote the motion of the end effector (foot); q_1 and q_2 to denote the rotation of the ankle about its axes; s_1, s_2, and s_3 to denote the length of extensible links; and ξ_1, ξ_2, and ξ_3 to denote the rotation of the extensible links about their second axes, the analytic Jacobian characterizing the motion level forward kinematics of 3UPS mechanism can be derived as

$$[\dot{x}\ \dot{y}\ \dot{z}\ \dot{\psi}_1\ \dot{\psi}_2\ \dot{\psi}_3]^T = J_{3UPS}\ [\dot{s}_1\ \dot{s}_2\ \dot{s}_3\ \dot{\xi}_1\ \dot{\xi}_2\ \dot{\xi}_3]^T \quad (1)$$

while the inverse Jacobian mapping of the spatial RR mechanism reads as

$$[\dot{q}_1\ \dot{q}_2]^T = J_{RR}^{-1}\ [\dot{x}\ \dot{y}\ \dot{z}\ \dot{\psi}_1\ \dot{\psi}_2\ \dot{\psi}_3]^T. \quad (2)$$

Given the forward kinematic map of the 3UPS mechanism and the inverse kinematic map of the spatial RR mechanism, the forward kinematics of 3UPS-RR mechanism can be constructed as

$$[\dot{q}_1\ \dot{q}_2]^T = J_{RR}^{-1}\ J_{3UPS}\ [\dot{s}_1\ \dot{s}_2\ \dot{s}_3\ \dot{\xi}_1\ \dot{\xi}_2\ \dot{\xi}_3]^T. \quad (3)$$

Inverse kinematics of 3UPS-RR mechanism can be calculated similarly. The kinematics of the 3UPS-RR characterize the mappings among sensor readings and the apparent rotation and torques at the ankle joint. Hence, these analyses can be used to determine RoM of the joints at ankle and to measure the maximum joint torque the patient can exert.

C. Kinematics of the 3UPS Mechanism

The 3UPS is an underactuated parallel mechanism and its the moving platform W possesses six independent DoF. To be able to utilize the exoskeleton as a clinical measurement device, the unique solutions to configuration and motion level kinematics of the 3UPS mechanism are necessitated. The configuration level kinematics of the 3UPS mechanism can be studied by forming three vector loop closure equations

$$\vec{r}^{ON_R} + \vec{r}^{N_RW_R} + \vec{r}^{W_RE} + \vec{r}^{EO} = \vec{0} \quad (4)$$
$$\vec{r}^{ON_S} + \vec{r}^{N_SW_S} + \vec{r}^{W_SE} + \vec{r}^{EO} = \vec{0} \quad (5)$$
$$\vec{r}^{ON_T} + \vec{r}^{N_TW_T} + \vec{r}^{W_TE} + \vec{r}^{EO} = \vec{0} \quad (6)$$

that can be solved for nine unknowns. Note that the relevant points used to form the vector loop equations are labeled in Figure 4. As with other parallel mechanisms, the solution of the inverse kinematics is trivial. On the other hand, determination of a unique solution to forward kinematic map is possible if measurements are available for six joint postions/angles of the 3UPS mechanism. To allow for feedback control, it is natural to have position measurements at the three prismatic joints of the device. Three extra sensors (encoders) are proposed to be instrumented, one encoder on each of the universal joints, so that end effector configuration of the underactuated mechanism can be uniquely determined by numerical solution of the nonlinear loop closure equations. Additional sensors utilized at the universal joints obligate the need for external sensors, such as motion trackers, to measure the complex 3-D motions of the foot.

Motion level kinematics of the 3UPS mechanism is studied by differentiating the three loop closure equations with respect to time to yield

$$^R\vec{v}^{W_R} + {}^N\vec{w}^R \times \vec{r}^{N_RW_R} + {}^N\vec{w}^W \times \vec{r}^{W_RE} - {}^N\vec{v}^E = \vec{0} \quad (7)$$
$$^S\vec{v}^{W_S} + {}^N\vec{w}^S \times \vec{r}^{N_SW_S} + {}^N\vec{w}^W \times \vec{r}^{W_SE} - {}^N\vec{v}^E = \vec{0} \quad (8)$$
$$^T\vec{v}^{W_T} + {}^N\vec{w}^T \times \vec{r}^{N_TW_T} + {}^N\vec{w}^W \times \vec{r}^{W_TE} - {}^N\vec{v}^E = \vec{0} \quad (9)$$

where $\vec{v}$ and $\vec{w}$ represent relative velocities and angular velocities, respectively. The relevant bodies are marked in Figure 4. The linear relationship between the time rate of change of end effector coordinates and the time rate of change of measured coordinates can be uniquely solved from these three independent vector equations to form the analytic Jacobian. The transpose of the analytic Jacobian is also of interest as it maps joint forces and torques to the end effector forces and torques.

The kinematics of the 3UPS is the mathematical mappings between sensor readings and the apparent configuration of and forces/torques at the ankle joints. Hence, this map can be used to determine the configuration of the foot and to measure the effective forces/torques acting on the foot.

D. Estimation of the Ankle Joint Axes

Kinematic structure of the human ankle is modeled a spatial serial kinematic chain with two revolute joints (RR) as depicted in Figure 5. To be able to use this model for estimation of the ankle parameters, the link lengths of this kinematic chain must be known along with the rotation axes of the revolute joints. Determination of the bone lengths is relatively straightforward as x-ray images of the ankle can be studied for reasonably accurate estimates. However, determination of the rotation axes is challenging since the motion of the ankle depend on the size and orientation of the foot bones, and the shape of articulated surfaces. Only course estimates of joint axes can be obtained studying the x-ray images. More accurate estimates of joint axes is desired to study the ankle motion and such estimates are made possible thanks to the data collected with the exoskeleton.

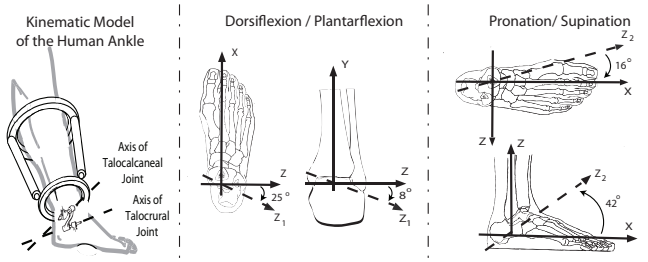

Fig. 5. Schematic representation of the kinematics of the human ankle (reconstructed from [38])

Given good estimations of the bone sizes, the axes of rotation of the revolute joints of the human ankle can be determined by instructing the patient to perform free RoM movements and by collecting encoder data from the prismatic joints and three *extra* sensors placed on the universal joints. As the data becomes available, the configuration level forward kinematics of the 3UPS mechanism is solved for the moving plate (foot) configurations at each instant of time. Once the foot configurations are recorded, the configuration level inverse kinematics of the two link RR manipulator, with the revolute joint axes unknown, is solved for the axes of revolute joints and the amount of rotation around these rotation axes.

When analyzed at a single instant in time, the inverse kinematics solution to the RR manipulator with unknown joint axes is essentially equivalent to the inverse kinematics of an SS manipulator, for which no unique solution exists. The problematic nature of the kinematic analysis of the SS manipulator arises from the fact that the rotation around the medial axis of the first link commands no change in the end effector pose, rendering the Jacobian map singular and obviating existence of infinitely many solutions to the inverse kinematics problem. However, a unique solution to the joint axes can still be sought in time, realizing that unlike for the SS manipulator, the joint axes need to stay fixed for the RR manipulator for data points collected at different instants of time. Hence, a nonlinear least squares algorithm can be utilized to converge to accurate estimates of joint axes when the estimation is initialized with the course estimates from x-ray images.

E. Numerical Example on the System Kinematics and the Estimation of the Joint Axes

Figure 6 depicts a sample configuration for the human-exoskeleton system with the 3UPS-RR structure. Link lengths for the ankle are chosen as 200mm, 33mm, and 40mm, representing the length of the upper mid-calf, the distance between upper ankle joint and the subtalar joint, and the distance from the subtalar joint to the center of the moving platform, respectively. The upper ankle and subtalar joint axes are modeled after Figure 5.

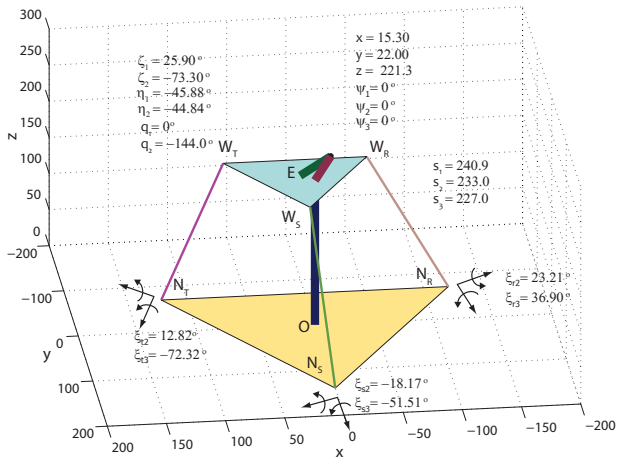

Fig. 6. Numerical solution to the kinematics of the 3UPS-RR mechanisms

Given the 3UPS encoder readings $\rho^T_{3UPS} = [s_1\ s_2\ s_3\ \xi_1\ \xi_2\ \xi_3]$, the configuration level forward kinematics of the 3UPS can be invoked to solve for the end effector configuration $\mathbf{x}^T_{3UPS} = [x\ y\ z\ \psi_1\ \psi_2\ \psi_3]$, where the orientation of the end effector is specified using Euler XYZ angles. Once more than one set of such encoder readings become available, a weighted nonlinear least-squares optimization routine can be utilized for finding optimal solution to the overdetermined system of nonlinear equations in the least-squares sense. The optimization routine is based on a modified Levenberg-Marquardt algorithm and is implemented in MATLAB.

For the example studied in Figure 6, the orientation of the moving platform is numerically calculated from the encoder values as depicted in the figure. If $\mathbf{A}^0_{RR} = [\zeta_1\ \zeta_2\ \eta_1\ \eta_2] = [20^\circ\ -70^\circ\ -40^\circ\ -40^\circ]$ are used as the initial guesses to initialize the nonlinear least squares estimation, the algorithm converges to $\mathbf{A}_{RR} = [\zeta_1\ \zeta_2\ \eta_1\ \eta_2] = [25.90^\circ\ -73.30^\circ\ -45.88^\circ\ -44.84^\circ]$ only after a few data sets are collected, where ζ_i and η_i, $i = 1, 2$ specify the orientations of the rotation axes of the revolute joints.

F. Implementation of a Reaction Torque Observer and Determination of the Ankle Impedance

Given the configuration and motion level forward and inverse kinematics of the coupled 3UPS-RR system and the dynamic properties of the exoskeleton, a robust position controller with a reaction torque observer can be implemented to characterize the dynamic properties of the

ankle. In particular, employing the robust position controller, the exoskeleton can command the ankle trace a desired trajectory, while disturbance forces due to the unknown dynamics of the ankle can be estimated during this motion. Block diagram of such a robust position controller is depicted in Figure 7. In the controller implementation, forces due to the known (modeled) dynamics of the exoskeleton is added to the system in a feedforward manner (through the model based disturbance estimator) to ensure that the disturbance acting on the system is solely due to the unknown dynamics of the ankle. Under such a control, the forces commanded by the controller is to counteract the unmodeled dynamics of the ankle. Hence, the actuator forces can be mapped to the joint torques at the ankle and assuming that all other disturbances are comparatively small, these torques provide a close estimate of the actual joint torques due to ankle dynamics.

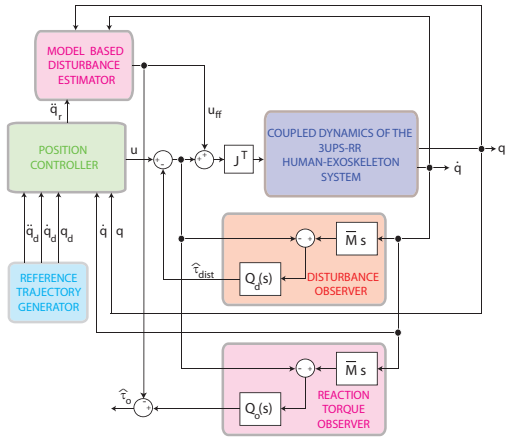

Fig. 7. Block diagram of the robust position controller with reaction torque observer

Figure 8 presents simulation results for the robust position controller when the upper ankle joint is moved to trace a 1Hz sinusoid with 25° amplitude and the subtalar joint is moved to trace a 1Hz sinusoid with 35° amplitude (see the top left plot). During these simulations, the unmodeled dynamics of the ankle are taken due to $b_u = 1.5$ N-s/rad, and $k_u = 50$ N-m/rad for the upper ankle joint, and $b_s = 1.0$ N-s/rad, and $k_s = 30$ N-m/rad for the subtalar joint. The actuators are assumed to behave a perfect force sources. In simulation, even with the large unmodeled dynamics, the tracking errors for the joints can be kept within 2° (see bottom left plot). The plots on the right present the motion of the linear actuators of the exoskeleton.

Figure 9 presents the reaction torque estimated by the controller, which are due to the unmodeled dynamics of the ankle. Since both the motion of the ankle and the torques due to the ankle dynamics can be measured about the joint axes at the desired frequencies, the ankle impedance can easily be estimated using standard parameter estimation techniques. Such estimates of the unmodeled ankle impedance about the joint axes are given in Figure 10. The estimated joint impedances can also be mapped to end effector (foot) impedance through a simple transformation dictated by the Jacobian map.

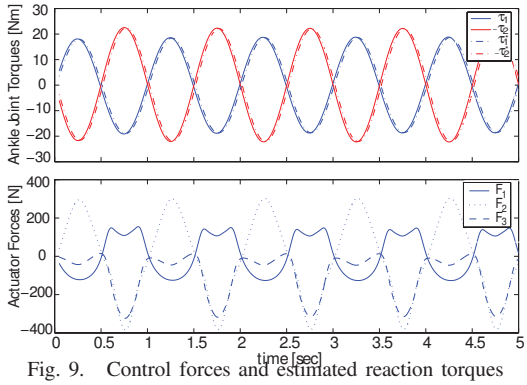

Fig. 9. Control forces and estimated reaction torques

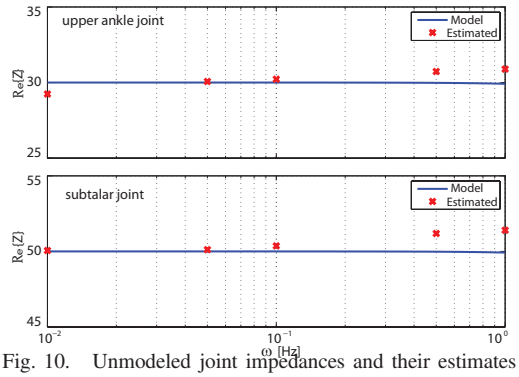

Fig. 10. Unmodeled joint impedances and their estimates

IV. CONCLUSIONS

The design, analyses, and clinical measurement use of a reconfigurable, parallel mechanism based ankle exoskeleton are presented. After identifying the relevant design criteria for several physical therapy exercises, kinematic structures of mechanisms that are best suited for these therapies are selected. Reconfigurability is embedded into the design such that a single device can be arranged as a 3UPS manipulator to administer RoM/strengthening exercises and as a 3RPS-R manipulator to support balance/proprioception exercises. Moreover, utilization of the exoskeleton as a clinical measurement tool to estimate dynamic parameters of the ankle is discusses and kinematic analysis and control of the device to determine ankle impedance are detailed.

V. ACKNOWLEDGMENTS

The authors gratefully acknowledge the TÜBİTAK 107M337, the Marie Curie International Reintegration 203324-REHAB-DUET grants, and the insightful comments of the reviewers.

REFERENCES

[1] H. Tropp and H. Alaranta, *Sports Injuries: Basic Principles of Prevention and Care, Proprioception and Coordination Training in Injury Prevention*. Oxford, 1993.

[2] M. Girone, G. Burdea, and M. Bouzit, "The Rutgers Ankle orthopedic rehabilitation interface," in *Proceedings of the ASME Haptics Symposium*, vol. 67, 1999, pp. 305–312.

[3] M. Girone, G. Burdea, M. Bouzit, V. Popescu, and J. Deutsch, "Orthopedic rehabilitation using the Rutgers Ankle interface," in *Proceedings of Virtual Reality Meets Medicine 2000*, 2000, pp. 89–95.

[4] ——, "A Stewart platform-based system for ankle telerehabilitation," in *Autonomous Robots 10*, 2001.

[5] R. Boian, M. Bouzit, G. Burdea, J. Lewis, and J. Deutsch, "Dual Stewart platform mobility simulator," in *Proceedings of the IEEE International Conference on Rehabilitation Robotics*, 2005, pp. 550–555.

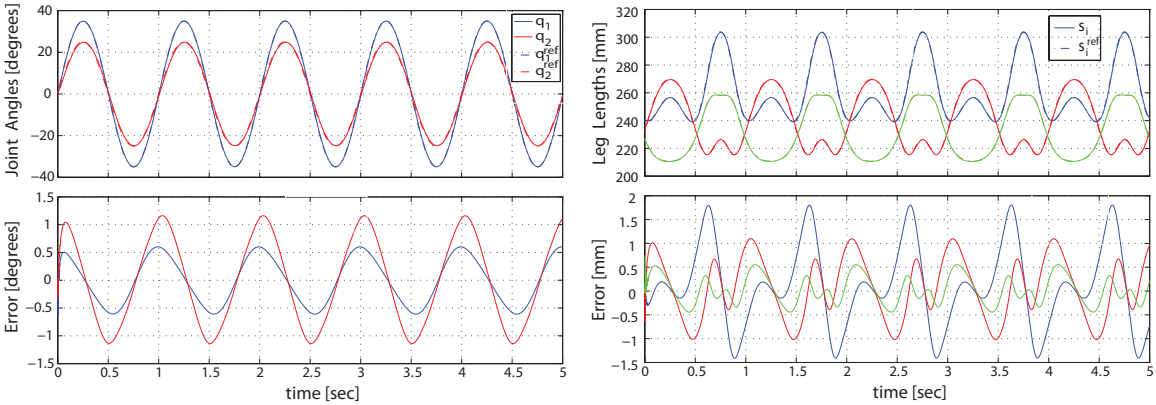

Fig. 8. Trajectory tracking of the ankle in the presence of unknown dynamic parameters

[6] J.S.Dai, T. Zhao, and C. Nester, "Sprained ankle physiotherapy based mechanism synthesis and stiffness analysis of a robotic rehabilitation device," in *Autonomous Robots*, vol. 16, 2004.

[7] A. Agrawal, S. K. Banala, S. K. Agrawal, and S. A. Binder-Macleod, "Design of a two degree-of-freedom ankle-foot orthosis for robotic rehabilitation," in *Proceedings of the IEEE International Conference on Rehabilitation Robotics*, 2005, pp. 41–44.

[8] C. E. Syrseloudis, I. Z. Emiris, C. N. Maganaris, and T. E. Lilas, "Design framework for a simple robotic ankle evaluation and rehabilitation device," in *International IEEE EMBS Conference*, 2008.

[9] J. Yoon, "A new family of hybrid 4-dof parallel mechanisms with two platforms and its application to a footpad device," *Journal of Robotic Systems*, vol. 22, no. 5, pp. 287– 298, 2005.

[10] J. Yoon, J. Ryu, and K. Lim, "A novel reconfigurable ankle rehabilitation robot for various exercise modes," *Journal of Robotic Systems (Currently Journal of Field Robotics)*, vol. 22, no. 1, pp. 15–33, 2006.

[11] A. Roy, H. I. Krebs, S. L. Patterson, T. N. Judkins, I. Khanna, L. W. Forrester, R. M. Macko, and N. Hogan, "Measurement of human ankle stiffness using the Anklebot," in *Proceedings of the IEEE International Conference on Rehabilitation Robotics*, 2007, pp. 356–363.

[12] K. Bharadwaj and T. Sugar, "Kinematics of a robotic gait trainer for stroke rehabilitation," *Robotics and Automation, 2006. ICRA 2006. Proceedings 2006 IEEE International Conference on*, pp. 3492–3497, May 2006.

[13] D. Ferris and C. Farley, "Interaction of leg stiffness and surface stiffness during human hopping," *American Physiological Society*, 1997.

[14] R. Kearney, R. Stein, and L. Parameswaran, "Identification of intrinsic and reflex contributions to human ankle stiffness dynamics," *IEEE Transactions On Biomedical Engineering*, vol. 44, no. 6, pp. 493–504, 1997.

[15] M.M.Mirbagheri, R.E.Kearney, and H.Barbeau, "Abnormal passive and intrinsic stiffness in the spastic ankle," in *Proceedings of the International Conference of the IEEE Engineering in Medicine and Biology Society, Vol. 20, No 5*, 1998.

[16] M. Mirbagheri, H. Barbeau, M. Ladouceur, and R. Kearney, "Intrinsic and reflex stiffness in normal and spastic, spinal cord injured subjects," *Exp Brain Res*, vol. 141, p. 446459, 2001.

[17] R. Lieber and J. Fride, "Spasticity causes a fundamental rearrangement of musclejoint interaction," *Muscle and Nerve*, vol. 25, pp. 265–270, 2002.

[18] T. Sinkjær and I. Magnussen, "Passive, intrinsic and reflex-mediated stiffness in the ankle extensors of hemiparetic patients," *Brain*, vol. 117, pp. 355–363, 1994.

[19] T. Sinkjær, E. Toft, K. Larsen, S. Andreassen, and H. Hansen, "Non-reflex and reflex mediated ankle joint stiffness in multiple sclerosis patients with spasticity," *Muscle and Nerve*, vol. 16, pp. 69–76, 1993.

[20] S. Lark, J. Buckley, S. Bennett, D. Jones, and A. Sargeant, "Joint torques and dynamic joint stiffness in elderly and young men during stepping down," *Clinical Biomechanics*, vol. 18, pp. 848–855, 2003.

[21] S. Chang and D. Rincon, "Biofeedback control ankle foot orthosis for stroke rehabilitation to improve gait symmetry," in *Conference on Recent Advances in Robotics, FCRAR*, 2006.

[22] P. Morasso and V. Sanguineti, "Direct measurement of human ankle stiffness during quiet standing: The intrinsic mechanical stiffness is insufficient for stability," *Journal of Physiology*, vol. 545.3, p. 10411053, 2002.

[23] C. Lin, M. Ju, S. Chen, and B. Pan, "A specialized robot for ankle rehabilitation and evaluation," *Journal of Medical and Biological Engineering*, vol. 28, no. 2, pp. 79–86, 2008.

[24] J. Hertel, "Functional anatomy, pathomechanics, and pathophysiology of lateral ankle instability," *Journal of Athletic Training*, vol. 37, pp. 364–375, 2002.

[25] J. Yoon and J. Ryu, "A novel reconfigurable ankle/foot rehabilitation robot," in *IEEE International Conference on Robotics and Automation*, 2005.

[26] ——, "Design, fabrication, and evaluation of a new haptic device using a parallel mechanism," *IEEE Transactions on Mechatronics*, vol. 6, no. 3, pp. 221–233, 2001.

[27] USA, Department of Defence, "Military handbook anthropometry of u.s. military personnel (metric)," February 1991, dOD-HDBK-743A.

[28] A. Gupta and M. K. O'Malley, "Design of a haptic arm exoskeleton for training and rehabilitation," *IEEE Transactions on Mechatronics*, vol. 11, no. 3, 2006.

[29] A. Gupta, V. Patoglu, M. K. O'Malley, and C. M. Burgar, "Design, control and performance of RiceWrist: A force feedback wrist exoskeleton for rehabilitation and training," *International Journal of Robotics Research, Special Issue on Machines for Human Assistance and Augmentation*, vol. 27, no. 2, pp. 233–251, 2008.

[30] R. Unal and V. Patoglu, "Optimal dimensional synthesis of force feedback lower arm exoskeletons," in *IEEE International Conference on Biomedical Robotics and Biomechatronics*, 2008.

[31] ——, "Optimal dimensional synthesis of a dual purpose haptic exoskeleton," in *Lecture Notes in Computer Science, Vol. 5024, Springer*, 2008.

[32] D. G. Wright, S. M. Desai, and W. H. Henderson, "Action of the Subtalar and Ankle-Joint Complex During the Stance Phase of Walking," *J Bone Joint Surg Am*, vol. 46, no. 2, pp. 361–464, 1964.

[33] J. Merlet, *Parallel Robots*, 2nd ed. Springer, 2006.

[34] A. Erdogan, A. C. Satici, and V. Patoglu, "Reconfigurable force feedback ankle exoskeleton for physical therapy," in *ASME/IFToMM International Conference on Reconfigurable Mechanisms and Robots*, 2009.

[35] R. Unal, G. Kiziltas, and V. Patoglu, "A multi-criteria design optimization framework for haptic interfaces," in *IEEE International Symposium on Haptic Interfaces for Virtual Environments and Teleoperator Systems*, 2008.

[36] ——, "Multi-criteria design optimization of parallel robots," in *IEEE International Conference on Cybernetics and Intelligent Systems and IEEE International Conference on Robotics, Automation and Mechatronics, CIS-RAM 2008*, 2008.

[37] A. K. D. I. M. Chen, S. H. Yeo, and G. Yang, "Task-oriented configuration design for reconfigurable parallel manipulators," *International Journal of Computer Integrated Manufacturing*, vol. 18, no. 7, pp. 615–634, 2005.

[38] R. Isman and V. Inman, "Anthropometric studies of the human foot and ankle," *Bulletin of Prosthesis Research*, vol. 10-11, pp. 97–129, 1969.